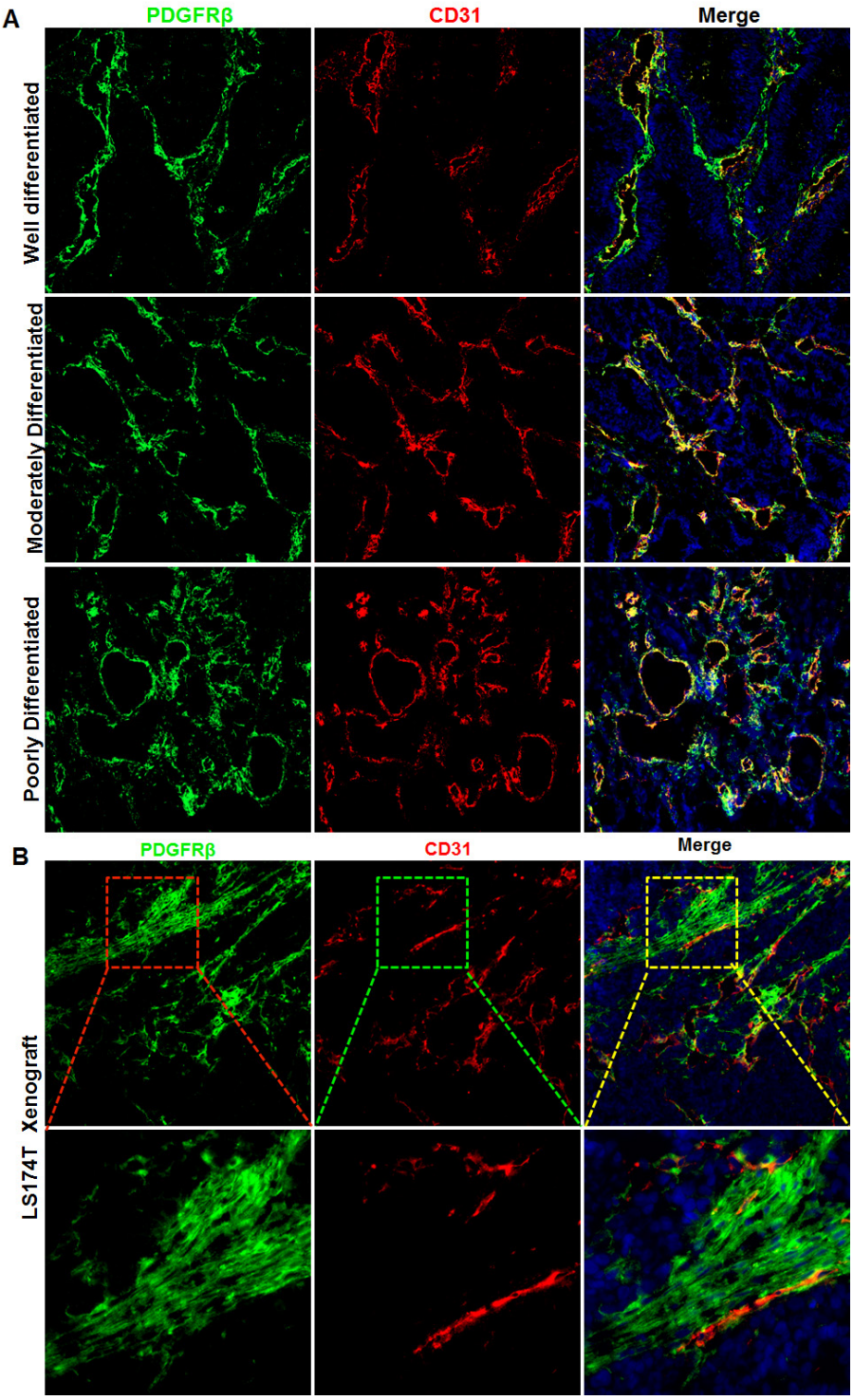

Figure S1 Expression of PDGFRβ in tumor tissues. **(A)** PDGFRβ expression in tumor tissues derived from patients with colon cancer at different stages. **(B)** PDGFRβ expression in stroma of tumor tissues derived from mice bearing LS174T tumor grafts. Tumor tissues were sectioned under frozen conditions and dually stained with anti-PDGFRβ antibody (green) and anti-CD31 antibody (red). The nuclei of cells were visualized using DAPI (blue). Original magnification, ×200.

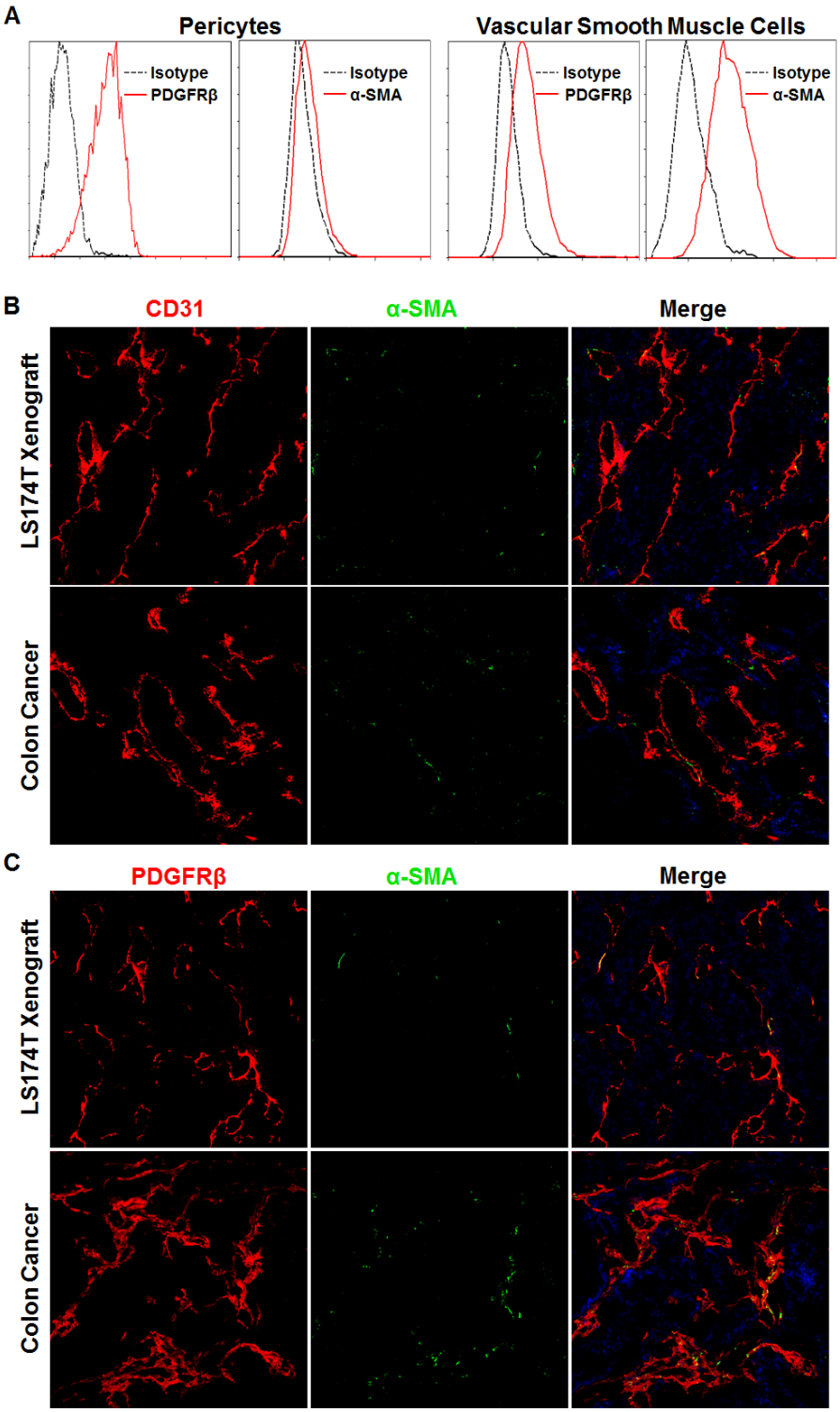

Figure S2 Characterization of microvessels of tumor tissues. **(A)** Expression of PDGFRβ and α-SMA in pericytes and vascular smooth muscle cells. **(B)** Co-localization of α-SMA and CD31 in microvessels of tumor tissues. **(C)** Co-localization of α-SMA and PDGFRβ in microvessels of tumor tissues. Original magnification, ×200.

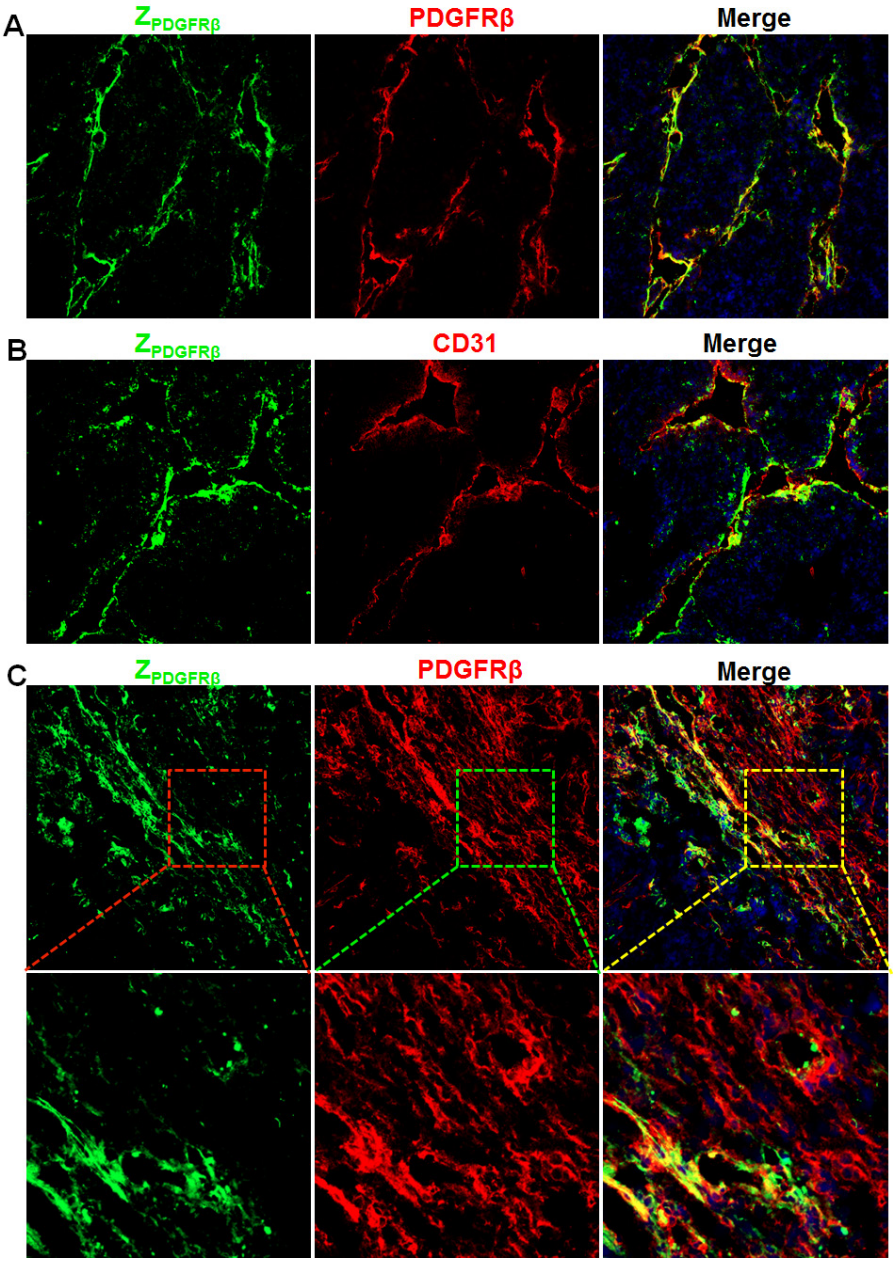

Figure S3 Distribution of $Z_{PDGFRβ}$ affibody on pericytes and fibroblasts. **(A)** Co-localization of $Z_{PDGFRβ}$ affibody and PDGFRβ in tumor parenchyma. **(B)** Co-localization of $Z_{PDGFRβ}$ affibody and CD31 in tumor parenchyma. **(C)** Co-localization of $Z_{PDGFRβ}$ affibody and PDGFRβ in tumor stroma. Mice bearing LS174T tumor xenografts were intravenously injected with FAM-labeled $Z_{PDGFRβ}$ affibody (green). The tumor xenografts were collected at 30 min post-injection. The sectioned tumor tissues were stained with anti-PDGFRβ antibody or anti-CD31 antibody. The nuclei of cells were visualized using DAPI (blue). Original magnification, ×200.

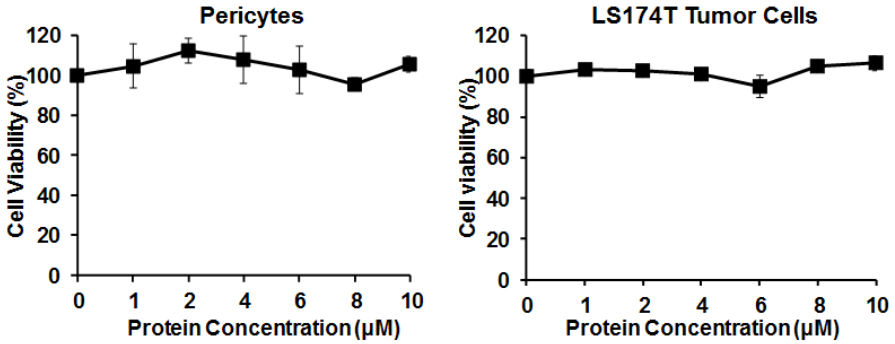

Figure S4 Cytotoxicity of $Z_{PDGFR\beta}$ affibody in pericytes and LS174T tumor cells. Cells (1×10^4/well) were treated with $Z_{PDGFR\beta}$ affibody at different concentrations (1-10 μM) overnight followed by measuring the viable cells using CCK-8. The viability of cell treated with PBS was considered as 100%.

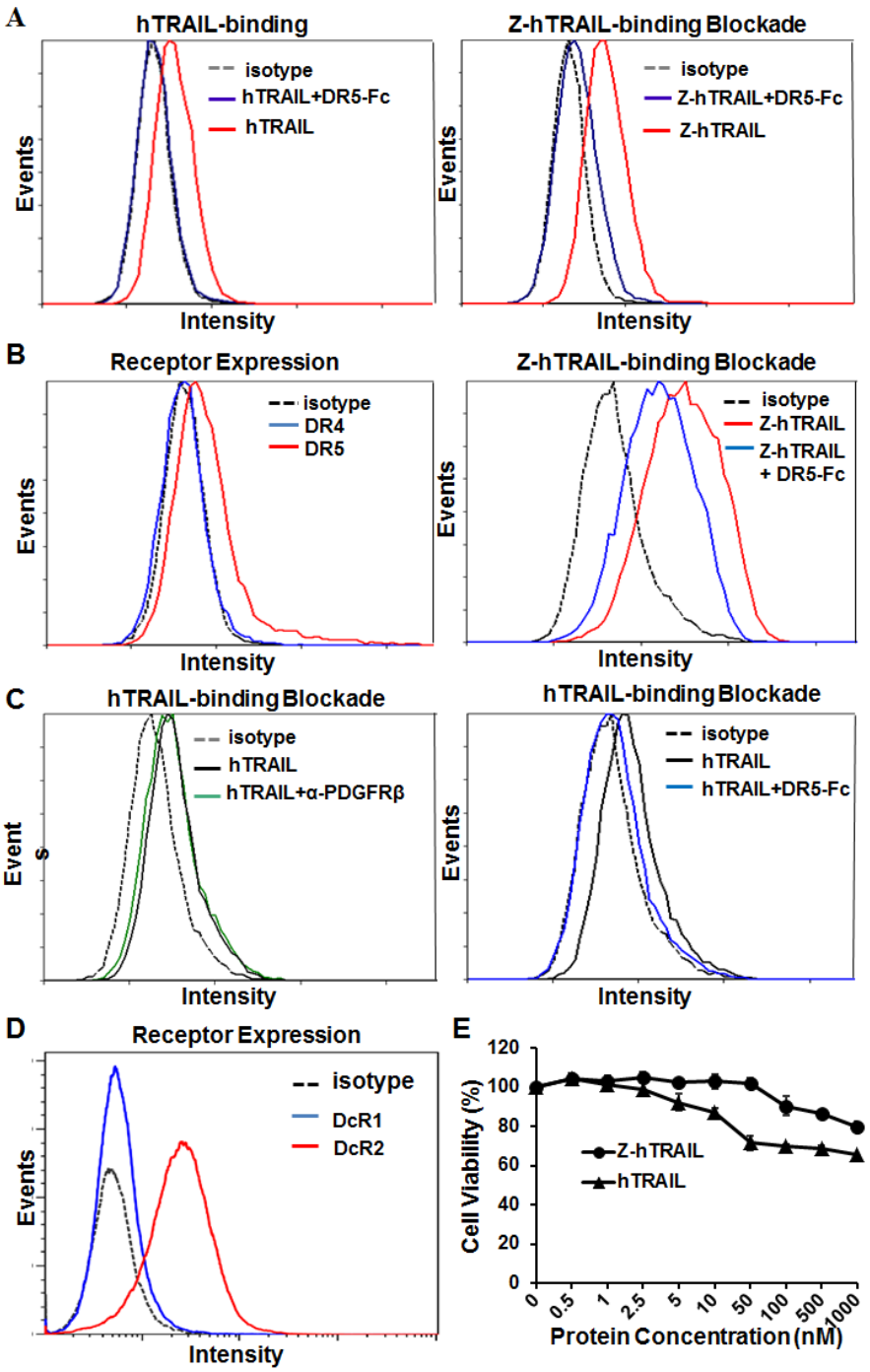

Figure S5 Binding of Z-hTRAIL on tumor cells and pericytes. **(A)** DR5-Fc-mediated blockade of cell binding of Z-hTRAIL to COLO205 tumor cells. **(B)** Expression of death receptor on pericytes and DR5-Fc-mediated blockade of pericyte-binding of Z-hTRAIL. **(C)** Anti-PDGFRβ antibody- and DR-Fc-mediated blockade of pericyte-binding of hTRAIL. **(D)** Expression of decoy receptors (DcR1 and DcR2) on pericytes. **(E)** Cytotoxicity of Z-hTRAIL and hTRAIL in pericytes.

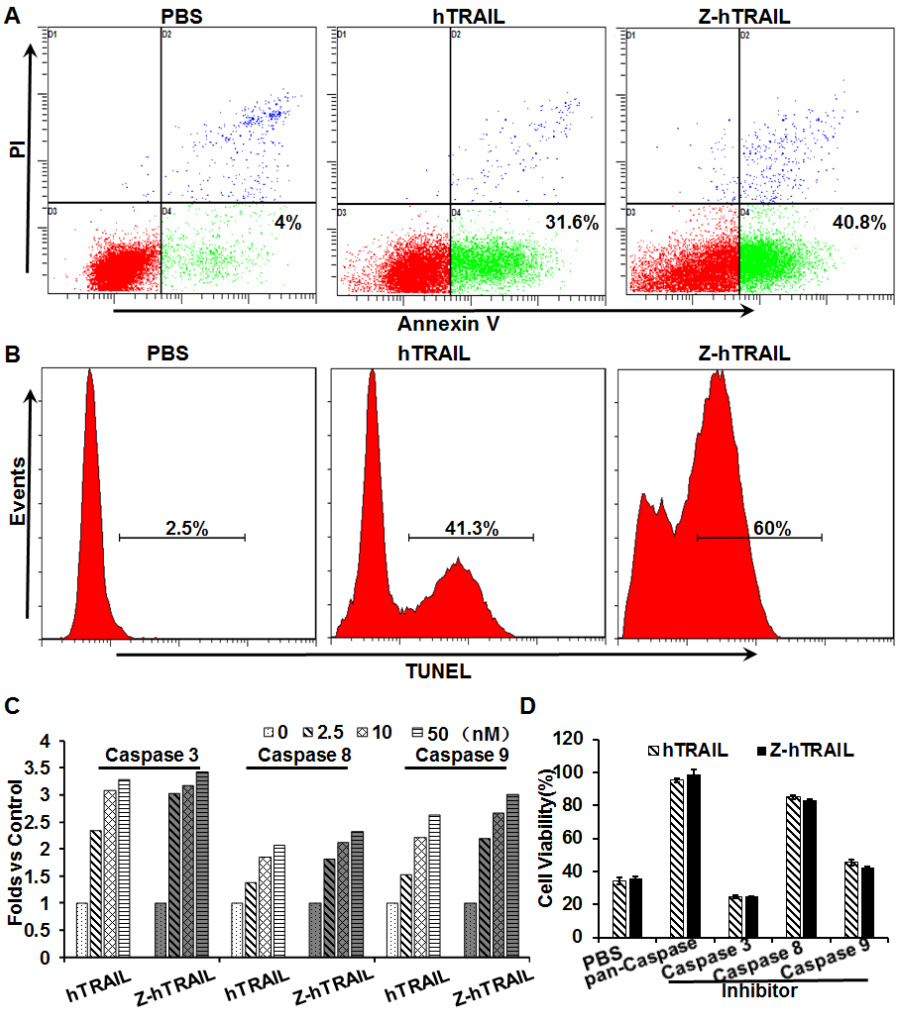

Figure S6 Apoptosis of COLO205 tumor cells induced by Z-hTRAIL and hTRAIL. **(A)** Annexin V/propidium iodide (PI) dual staining assay. Cells (4×10^5) were treated with Z-hTRAIL or hTRAIL (0.5 nM) for 2 h at 37°C. Subsequently, the cells were dually stained with Annexin V and PI followed by flow cytometry analysis. Annexin V-/PI+ cells were considered apoptotic cells. **(B)** TUNEL staining assay. Cells (1×10^6) were treated with Z-hTRAIL or hTRAIL (2.5 nM) at 37°C for 2 h. Subsequently, the cells were dually stained with TUNEL solution prior to flow cytometry. **(C)** Caspase activity assay. Cells (6×10^6) were treated with different concentrations (0-50 nM) of Z-hTRAIL or hTRAIL at 37°C for 2 h. Subsequently, the activities of caspase 3, 8, and 9 were measured using specific chromogenic substrates. The activity of caspases in protein-treated cells was expressed as fold vs PBS-treated cells. **(D)** Caspase inhibitor-mediated reduction of cytotoxicity in tumor cells. Cells (1×10^4 cells/well) were seeded in 96-well plates and preincubated with caspase 3-, 8-, and 9-specific inhibitors or a pan-caspase inhibitor (20 μM) at 37°C for 2 h prior to addition of Z-hTRAIL (4 nM) or hTRAIL (25 nM). After treatment at 37°C overnight, the surviving cells were examined using CCK-8 solution.

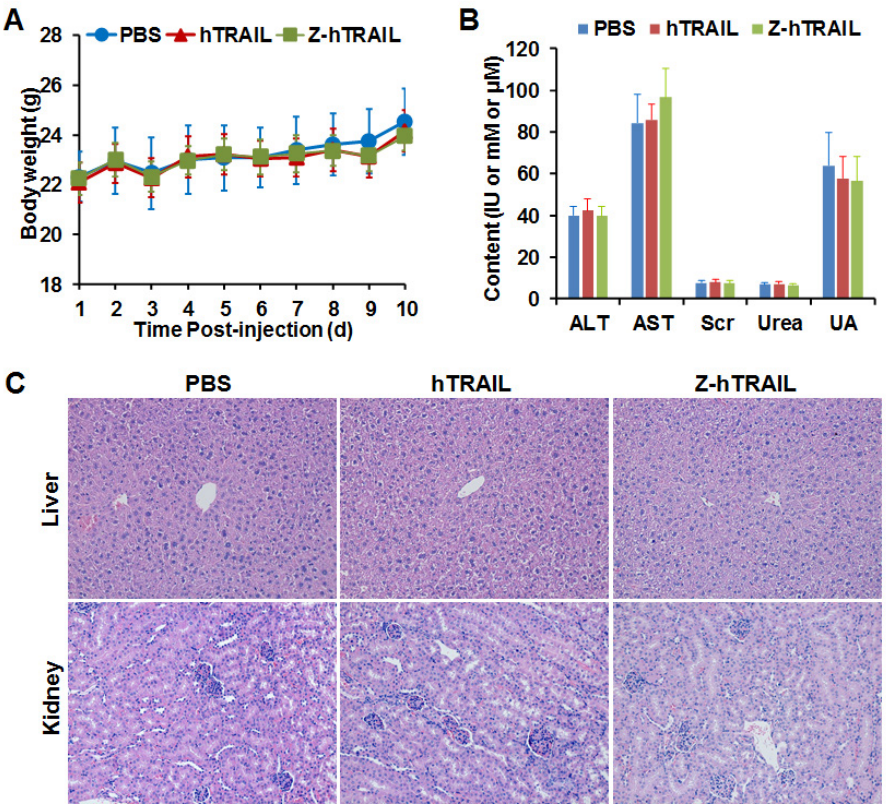

Figure S7 Acute cytotoxicity of Z-hTRAIL. **(A)** Body weight of mice. **(B)** Blood biochemical indicators for function of liver (ALT and AST) and kidney (Scr, Urea and UA) of mice. **(C)** Structure of liver and kidney of mice illustrated by H&E staining. Original magnification, ×200.